Electron-nitrogen scattering in dilute nitrides

M. P. Vaughan* and B. K. Ridley
Department of Electronic Systems Engineering, University of Essex, Colchester CO4 3SQ, United Kingdom
(Received 16 October 2006; revised manuscript received 9 January 2007; published 8 May 2007)

An n-band Hamiltonian for a dilute nitride system is derived using Anderson's many-impurity model. Using this, an energy-dependent relaxation time for electron-nitrogen scattering is derived, compared, and contrasted to existing theoretical models for the mobility in dilute nitrides. The nonparabolicity of the band structure creates problems when integrating functions of energy over the bands, so modified forms of the density of states in three dimensions and two dimensions that conserve the number of states are derived from the Green's function of the system. The bulk mobility for GaN_xAs_{1-x} is calculated for the case of isolated nitrogen and nitrogen pair environments as a function of carrier and nitrogen concentration. In the highly degenerate case, the calculated room-temperature mobilities, excluding other scattering processes, are in good agreement with reported experimental determinations.

DOI: 10.1103/PhysRevB.75.195205 PACS number(s): 71.55.Eq, 72.80.Ey, 72.20.Dp, 72.20.Fr

I. INTRODUCTION

The use of III-V semiconductors, such as GaInAs, doped with dilute concentrations of nitrogen has attracted a great deal of interest for device applications due to the large bowing of the energy gap[1,2] with nitrogen content x and the possibility of lattice matching to GaAs substrates. A possible drawback for such applications is the large drop in mobility observed[3–7] as nitrogen is added, and this provides the motivation for a theoretical understanding of the mechanisms limiting carrier transport in dilute nitrides.

It is well known that nitrogen forms a deep-level state in GaAs (Refs. 8–10) or GaP,[11,12] which in GaAs is resonant with the conduction band (here, "deep" refers to the nature of the trapping potential rather than implying the energy level lies in the energy gap—see Hjalmarson *et al.*[13] for a theoretical discussion). Band-structure calculations using the empirical pseudopotential method[14–18] or tight-binding[19–23] (TB) calculations show that this nitrogen state is highly localized. Moreover, with increasing nitrogen content, additional localized states due to nitrogen clusters have been both predicted and observed.[9,10] The restructuring of the conduction band can be understood as being due to a mixing of these localized states with the extended matrix semiconductor states.

The simplest model based on this interpretation is the band-anticrossing (BAC) model due to Shan *et al.*,[24] in which an isolated nitrogen state hybridizes with the extended host states, splitting the conduction band into two separate bands and greatly perturbing the dispersion relations. A three-band model incorporating nitrogen (N-N) pairs was proposed along similar lines by Lindsay,[25,26] and later, O'Reilly *et al.* developed a more general n-band model consistent with TB calculations in which the eigenstates of the system can be represented by a linear combination of isolated nitrogen states (LCINS) and the host eigenstates.[20–23] A common feature of all these models is a predicted increase in the effective mass (despite the reduction in band gap) and increased nonparabolicity of the dispersion relations. These effects alone, however, do not account for the severe drop in mobility, and we must therefore consider enhanced carrier scattering due to the nitrogen states.

The first model to specifically address the problem of the electron scattering in dilute nitrides was developed by Fahy and O'Reilly,[27] who derived a scattering cross section from the S-matrix element for an ultradilute system. Initially, these authors considered only isolated nitrogen states but later developed their model to include N-N pairs.[28] Subsequently, Fahy *et al.* developed a more sophisticated model based on resonant scattering using the LCINS representation.[29,30] An alternative approach was pursued by Wu *et al.*,[31] who had derived the two-band BAC model from the Green's function for the Anderson many-impurity model[32] in the coherent potential approximation (CPA).[33]. A novel feature of their model was that the energy eigenvalues now acquired an imaginary component, interpreted as an energy broadening. In a subsequent paper,[34] Wu *et al.* suggested that this broadening should imply a finite electron lifetime via the uncertainty principle and took this to play the role of a relaxation time in mobility calculations. Good agreement with experimental mobilities was found using this model when the semiconductor was highly degenerate.

Although these models may seem quite disparate on the face of it, the formal similarity between the LCINS model for a single impurity and the CPA approach has already been pointed out by Fahy *et al.* In Sec. II, we find a more general Green's function for the Anderson model and use this to derive a variant of the LCINS model, differing principally in that the energy eigenvalues are complex. We then use this Hamiltonian to derive a scattering rate in Sec. III. This is found to have a similar form to the resonant scattering rate in the model of Fahy *et al.*,[29,30] although our model exhibits a different energy dependence and for a single impurity involves no approximations. The Green's function is then used to derive analytical forms for the density of states in Sec. IV, which remain well behaved even close to the impurity energy levels. Finally, we calculate the mobility for a dilute nitride system for two-band and three-band models in Sec. V.

II. n-BAND MODEL

In the many-impurity Anderson model,[32] the Hamiltonian can be written as

$$H = H_0 + V, \tag{1}$$

where H_0 is a sum of two terms describing the energies of extended and localized states, labeled by wave vector $\mathbf{k}$ and position vector $\mathbf{j}$, respectively, as follows:

 ©2007 The American Physical Society

$$H_0 = \sum_{\mathbf{k}} E_{\mathbf{k}} b_{\mathbf{k}}^{+} b_{\mathbf{k}} + \sum_{\mathbf{j}} E_{\mathbf{j}} b_{\mathbf{j}}^{+} b_{\mathbf{j}}. \quad (2)$$

The b_n^+ and b_n denote creation and annihilation operators, respectively. The second term in Eq. (1) represents an interaction between the extended and localized states as follows:

$$V = \frac{1}{\sqrt{N_C}} \sum_{\mathbf{j},\mathbf{k}} \{ e^{i\mathbf{k}\cdot\mathbf{j}} V_{\mathbf{kj}} b_{\mathbf{k}}^{+} b_{\mathbf{j}} + e^{-i\mathbf{k}\cdot\mathbf{j}} V_{\mathbf{kj}}^{*} b_{\mathbf{j}}^{+} b_{\mathbf{k}} \}, \quad (3)$$

where N_C is the number of primitive cells in the crystal and the $V_{\mathbf{kj}}$ characterize the hybridization strength.

In order that Eq. (1) gives the Hamiltonian of the unperturbed system (i.e., $H_0|n\rangle = E_n|n\rangle$, where n labels either a $\mathbf{k}$ or a $\mathbf{j}$ state), the state vectors $|n\rangle$ must form a complete orthonormal set. Inspecting the action of V, we find

$$\langle \mathbf{k}'|V|\mathbf{k}\rangle = 0, \quad \langle \mathbf{j}'|V|\mathbf{j}\rangle = 0,$$

$$\langle \mathbf{j}|V|\mathbf{k}\rangle = e^{-i\mathbf{k}\cdot\mathbf{j}} \frac{V_{\mathbf{kj}}^{*}}{\sqrt{N_C}}, \quad \langle \mathbf{k}|V|\mathbf{j}\rangle = e^{i\mathbf{k}\cdot\mathbf{j}} \frac{V_{\mathbf{kj}}}{\sqrt{N_C}}. \quad (4)$$

It is further assumed that different localized states do not interact in any way. In particular, products such as $\langle \mathbf{j}'|V^2|\mathbf{j}\rangle$ are zero whenever $\mathbf{j}' \neq \mathbf{j}$. The Green's function for the system is then found to be[35]

$$G_{\mathbf{kk}} = \left\{ E - E_{\mathbf{k}} - \frac{1}{N_C} \sum_{\mathbf{j}} \frac{|V_{\mathbf{kj}}|^2}{E - E_{\mathbf{j}} - S_{\mathbf{j}}} \right\}^{-1}, \quad (5)$$

where $S_{\mathbf{j}} = (1/N_C)\Sigma_{\mathbf{k}} G_{\mathbf{kk}}^0 |V_{\mathbf{kj}}|^2$. Following Anderson, this can be turned into an integral over $\mathbf{k}$ states, yielding an energy shift and an imaginary term, interpreted as an energy broadening. Absorbing the energy shift into $E_{\mathbf{j}}$, the broadening is

$$\Delta_{\mathbf{j}} \approx \pi N_0(E_{\mathbf{j}}) \langle V_{\mathbf{kj}}^2 \rangle, \quad (6)$$

where N_0 is the density of states of the host semiconductor and the angular brackets indicate an averaging of $|V_{\mathbf{jk}}|^2$. We assume that the $\mathbf{k}$ dependence of the interaction term is weak and drop its $\mathbf{k}$ subscript in Eq. (5). The Green's function can then be written as

$$G_{\mathbf{kk}} = \left\{ E - E_{\mathbf{k}} - \frac{1}{N_C} \sum_{\mathbf{j}} \frac{V_{\mathbf{j}}^2}{E - E_{\mathbf{j}} + i\Delta_{\mathbf{j}}} \right\}^{-1}. \quad (7)$$

From the poles of Eq. (7), we can construct the n-band Hamiltonian

$$H = \begin{bmatrix} E_M(\mathbf{k}) & V_1/\sqrt{N_C} & V_2/\sqrt{N_C} & \cdots & V_{n-1}/\sqrt{N_C} \\ V_1/\sqrt{N_C} & E_1 - i\Delta_1 & 0 & \cdots & 0 \\ V_2/\sqrt{N_C} & 0 & E_2 - i\Delta_2 & \cdots & 0 \\ \vdots & \vdots & \vdots & \ddots & 0 \\ V_{n-1}/\sqrt{N_C} & 0 & 0 & 0 & E_{n-1} - i\Delta_{n-1} \end{bmatrix}. \quad (8)$$

[Essentially, we can show that the solution of the characteristic equation $|H-E|=0$ reproduces the poles of Eq. (7).[35]] Here, we have put $E_{\mathbf{k}} = E_M(\mathbf{k})$ to highlight the fact that this is the energy of the host semiconductor. This Hamiltonian closely resembles the LCINS model except for two differences. Firstly, in this model, the $|\mathbf{j}\rangle$ states are all orthogonal to each other, whereas in the LCINS model, they are not. Secondly, the solutions of the characteristic equation for this Hamiltonian yield complex energy eigenvalues, the imaginary part being interpreted as energy broadening. The first of these differences is not likely to be too significant, since, by definition, we are dealing with isolated impurities and the spatial overlap between them will be negligible. The principal significance of this approach, which introduces the broadening concomitantly, is that it allows us to derive integrable densities of states, as will be discussed in Sec. IV. The effect of the broadening itself on the band structure is actually to weaken the hybridization of extended and localized states, bringing the real dispersion relations closer to those of the host semiconductor [see Eq. (7), noting that the Green's function of the unperturbed system is $G_{\mathbf{kk}}^0 = (E - E_{\mathbf{k}})^{-1}$].

It will be convenient to separate the complex energy into real and imaginary components, putting $E \to E + i\Delta(E)$. The matrix semiconductor energy (which is always real) can now be written as a function of the real energy E as follows:

$$E_M(E) = \frac{1}{N_C} \sum_{\mathbf{j}} \frac{V_{\mathbf{j}}^2 (E_{\mathbf{j}} - E)}{(E_{\mathbf{j}} - E)^2 + [\Delta_{\mathbf{j}} - \Delta(E)]^2} + E \equiv \gamma(E). \quad (9)$$

Note that while this can be derived from the solution to the characteristic equation $|H-E|=0$, it is much easier to see how it can be found from the poles of Eq. (7) by applying the condition that the imaginary part of E_M [$E_{\mathbf{k}}$ in Eq. (7)] is zero. The $\gamma(E)$ function defined above proves to be highly useful in the description of the dispersion relations. In the simplest case (when E_M is parabolic), we have

$$\gamma(E) = \frac{\hbar^2 k^2}{2m_0^*}, \quad (10)$$

where m_0^* is the effective mass of the matrix semiconductor. $\gamma(E)$ also serves to define the extent of the bands in the model, being positive over a band and negative in the gaps.

The eigenfunctions $|\psi_{\mathbf{k}}\rangle$ of Eq. (8) can be expanded in terms of the extended matrix semiconductor state $|\phi_{\mathbf{k}}\rangle$ corresponding to E_M and the localied states $|\mathbf{j}\rangle$ as follows:

$$|\psi_{\mathbf{k}}\rangle = \alpha_M |\phi_{\mathbf{k}}\rangle + \sum_{\mathbf{j}} \alpha_{\mathbf{j}} |\mathbf{j}\rangle, \quad (11)$$

where $\alpha_M = \langle \phi_{\mathbf{k}} | \psi_{\mathbf{k}} \rangle$ and $\alpha_{\mathbf{j}} = \langle \mathbf{j} | \psi_{\mathbf{k}} \rangle$. The squared modulus $|\alpha_M|^2$ is often referred to as the fractional Γ character in the literature, and in this model, it is found to be

$$|\alpha_M|^2 = \left\{ \frac{1}{N_C} \sum_{\mathbf{j}} \frac{V_{\mathbf{j}}^2}{(E_{\mathbf{j}} - E)^2 + [\Delta_{\mathbf{j}} - \Delta(E)]^2} + 1 \right\}^{-1}. \quad (12)$$

Note that in the limit of taking all the broadenings $\Delta_{\mathbf{j}} \to 0$, this expression is just the inverse of $d\gamma(E)/dE$, since the broadening $\Delta(E)$ is just a weighted sum of the $\Delta_{\mathbf{j}}$ as follows:

$$\Delta(E) = \sum_{\mathbf{j}} |\alpha_{\mathbf{j}}|^2 \Delta_{\mathbf{j}}. \quad (13)$$

One further result we need to extract from the n-band model is the projection of the $|\mathbf{j}\rangle$ states on $|\psi_{\mathbf{k}}\rangle$,

$$|\alpha_{\mathbf{j}}|^2 = \frac{|\alpha_M|^2}{N_C} \frac{V_{\mathbf{j}}^2}{(E-E_{\mathbf{j}})^2 + [\Delta(E) - \Delta_{\mathbf{j}}]^2}. \tag{14}$$

III. THE SCATTERING RATE

The scattering rate at wave vector $\mathbf{k}$ can be determined from the S-matrix element

$$S(k,k) = \langle \mathbf{k} | V | \psi(\mathbf{k}) \rangle, \tag{15}$$

where $|\mathbf{k}\rangle$ is an extended state of the host semiconductor (an eigenvector of the first term in the Anderson Hamiltonian) and V is the interaction term given by Eq. (3). For a single impurity, this yields

$$|S(k,k)|^2 = \frac{V_{\mathbf{j}}^2}{N_C} |\alpha_{\mathbf{j}}|^2 = \frac{|\alpha_M(E)|^2}{N_C^2} \frac{V_{\mathbf{j}}^4}{(E-E_{\mathbf{j}})^2 + [\Delta(E) - \Delta_{\mathbf{j}}]^2}. \tag{16}$$

This has a very similar form to the scattering rate obtained by Fahy *et al.*[29,30] (which is strictly Lorentzian). This should not be too surprising given the similarity of the assumptions made and the Hamiltonian used. However, we note that our model has a different energy dependence arising from the inclusion of the fractional Γ character and the energy-dependent broadening. We also note that we have not made any approximations in the calculation of $|\alpha_{\mathbf{j}}|^2$.

From Eq. (15), we can obtain a scattering rate $w(E)$ [or relaxation time $\tau(E)$] as follows:

$$w(E) = \frac{1}{\tau(E)} = \frac{2\pi}{\hbar} |S(k,k)|^2 V_C N(E), \tag{17}$$

where V_C is the crystal volume and $N(E)$ is the density of states per unit volume. Note that for a single impurity, we find that $\tau^{-1}(E) \propto |\alpha_{\mathbf{j}}|^2 \propto \Delta(E)$ [from Eq. (13)], in the spirit of the model of the mobility of Wu *et al.*[34]

For more than one impurity, use of Eq. (15) with Eq. (3) gives rise to interference terms. We shall assume that each site scatters independently, so instead of using the full interaction term V in $S(k,k)$, we sum the S-matrix elements for each impurity site, giving

$$\begin{aligned} w(E) &= \sum_{\mathbf{j}} w_{\mathbf{j}}(E) \\ &= \frac{2\pi}{\hbar} \frac{V_C}{N_C^2} |\alpha_M|^2 \sum_{\mathbf{j}} \frac{V_{\mathbf{j}}^4}{(E-E_{\mathbf{j}})^2 + [\Delta(E) - \Delta_{\mathbf{j}}]^2} N(E). \end{aligned} \tag{18}$$

(Equivalently, we could use the full Hamiltonian and neglect the interference terms.) We now make a simplification by assuming that all impurities of a similar environment (e.g., an isolated N atom or a N-N pair) have the same energy, broadening, and interaction energy. The summation in Eq. (18) can then be turned into a summation over *types* of environment, which we shall label with the italic subscript j. Also, noting that the volume of a primitive cell in a zinc-blende crystal is $V_C/N_C = a_0^3/4$, where a_0 is the lattice constant, Eq. (18) becomes

$$w(E) = \frac{\pi}{2\hbar} a_0^3 |\alpha_M|^2 \sum_j \frac{V_j^4 x_j}{(E-E_j)^2 + [\Delta(E) - \Delta_j]^2} N(E), \tag{19}$$

where x_j is the concentration of the jth impurity environment.

IV. THE DENSITY OF STATES

Previously, we noted that the density of states calculated from the dispersion relations of the BAC (or n-band) model using the normal formula was problematic.[36] Specifically, deriving the densities of states from the dispersion relations in Eq. (10) gives us formulas of the form $N_{3D}(E) \sim \gamma^{1/2}(E)/d\gamma(E)/dE$ and $N_{2D}(E) \sim d\gamma(E)/dE$. Integrating these expressions over energy, we find that the number of states with an energy less than E is predicted to be proportional to $\gamma^{3/2}(E)$ in three dimensions and $\gamma(E)$ in two-dimensions. However, from Eq. (9), we see that $\gamma(E)$ approaches infinity near any impurity energy, implying an infinite number of states in the system. Apart from being physically invalid, this makes the mathematical calculation of quantities that rely on an integration over energy (notably carrier concentration) impossible.

Of course, there is a degree of artificiality imposed here, since in Eq. (9) we are implicitly assuming spherical energy bands. This assumption together with any description of the dispersion relations close to a Brillouin-zone boundary will inevitably produce singularities in the densities of states (although these may still be integrable). However, in GaNAs, the impurity levels occur quite low in the conduction band where spherical energy bands are still a realistic assumption and the issue is of a different nature to dealing with Van Hove singularities.

The problem can be addressed by deriving the density of states from the imaginary part of the Green's function using[31]

$$N(E) = -\frac{1}{\pi} \mathrm{Im} \int G_{\mathbf{kk}} N_0(E_{\mathbf{k}}) dE_{\mathbf{k}}, \tag{20}$$

where N_0 is the matrix semiconductor density of states. If we now define

$$\Omega(E) = -\sum_j \frac{V_j^2 x_j \Delta_j}{(E-E_j)^2 + \Delta_j^2} \tag{21}$$

and

$$\Gamma(E) = E - \sum_j \frac{V_j^2 x_j (E-E_j)}{(E-E_j)^2 + \Delta_j^2}, \tag{22}$$

we find that the imaginary part of $G_{\mathbf{kk}}$ is

$$\mathrm{Im}\, G_{\mathbf{kk}} = -\frac{\Omega(E)}{[\Gamma(E) - E_M]^2 + \Omega^2(E)}. \tag{23}$$

Inserting this into Eq. (20), we find the three-dimensional (3D) and two-dimensional (2D) densities of states to be

$$N_{3D}(E) = -\frac{(2m_0^*)^{3/2}}{4\pi^2\hbar^3}\Omega(E)(2\{[\Gamma^2(E)+\Omega^2(E)]^{1/2}-\Gamma(E)\})^{-1/2} \tag{24}$$

and

$$N_{2D}(E) = \frac{m_0^*}{2\pi\hbar^2}\sum_n\left[\frac{1}{2}-\frac{1}{\pi}\arctan\left(\frac{\Gamma(E)-E_n}{\Omega(E)}\right)\right], \tag{25}$$

where E_n is the energy at the bottom of the nth subband. Note that m_0^* is the *matrix semiconductor* effective mass. These expressions can be simplified by taking the limit as all the broadenings $\Delta_j\rightarrow 0$. However, rather than tackling each case separately, it is more useful to take the limit of the imaginary part of the Green's function before we perform the integration in Eq. (20). Firstly, we find that $\Gamma(E)\rightarrow\gamma(E)$, while $\Omega(E)\rightarrow 0$. Thus,

$$-\frac{1}{\pi}\lim_{\Delta_j\to 0}\mathrm{Im}\,G_{\mathbf{kk}} = \frac{1}{\pi}\lim_{\Omega\to 0}\frac{\Omega(E)}{[\gamma(E)-E_M]^2+\Omega^2(E)} = \delta(\gamma(E)-E_M). \tag{26}$$

This gives us a general prescription for finding the density of states as long as we know the density of states in host semiconductor, since we just replace E_M with $\gamma(E)$. The 3D density of states is then

$$\lim_{\Delta_j\to 0} N_{3D}(E) = \frac{(2m_0^*)^{3/2}}{4\pi^2\hbar^3}\gamma^{1/2}(E), \tag{27}$$

while the 2D density of states becomes

$$\lim_{\Delta_j\to 0} N_{2D}(E) = \frac{m_0^*}{2\pi\hbar^2}\sum_n \theta[\gamma(E)-E_n], \tag{28}$$

where $\theta(x)$ is the Heaviside step function. Examples of the densities of states for a three-band model are shown in Figs. 1 and 2. Note that while we see the emergence of singularities in the 3D density of states when $\Delta_i=0$, the density of states remains integrable. As an initial justification of this statement, consider that close to an impurity energy E_i, the leading term in a series expansion of Eq. (27) will be proportional to $(E_i-E)^{-1/2}$ [see Eq. (9)], which integrates to $2(E_i-E)^{1/2}$.

In the 2D case when $\Delta_i=0$, we find that the density of states in a single subband has the same magnitude as in the matrix semiconductor, just shifted down in energy. This is a somewhat surprising result since given a singularity in the 3D case, we might expect something similar in 2D. In fact, once we take the summation over the subbands into account, this is indeed what we get. Firstly, let us consider the case of an infinite quantum well of width d. In the limit $d\rightarrow\infty$, we can turn the summation in Eq. (28) into an integral via

$$\sum_n \rightarrow \frac{d}{\pi}\int_0^\infty dk_n = \frac{d}{\pi}\frac{(2m^*)^{1/2}}{2\hbar}\int_0^\infty E_n^{-1/2}dE_n,$$

since $E_n=\hbar^2k_n{}^2/2m^*$. Now, the action of the step function in Eq. (28) means that the integral is only nonzero when $\gamma(E) > E_n$, so we have

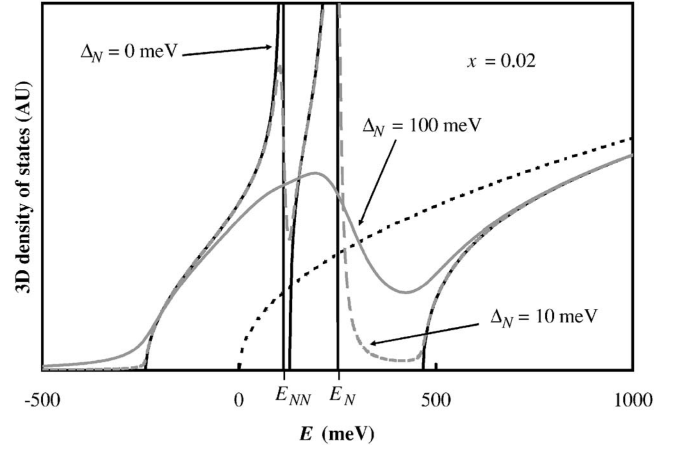

FIG. 1. 3D density of states for GaNAs calculated from the imaginary part of the Green's function using a three-band model (in this calculation, the broadenings on the two energy levels are taken to be equal). The black dotted line shows the GaAs density of states (the origin $E=0$ is taken at the matrix semiconductor band edge). Note that in the limit of taking all the broadenings to zero, the density of states becomes infinite at the impurity energies E_N and E_{NN}.

$$\lim_{d\to\infty}\frac{m^*}{2\pi\hbar^2}\sum_n\theta[\gamma(E)] = d\frac{(2m^*)^{3/2}}{8\pi^2\hbar^3}\int_0^{\gamma(E)}E_n^{-1/2}dE_n = d\frac{(2m^*)^{3/2}}{4\pi^2\hbar^3}\gamma^{1/2}(E) = N_{3D}(E)d,$$

which reproduces the 3D density of states.

Figure 3 offers a little more insight into the 2D case for a well of finite width (here, we only consider the two-band model for clarity). Since $\gamma(E)$ becomes large as E ap-

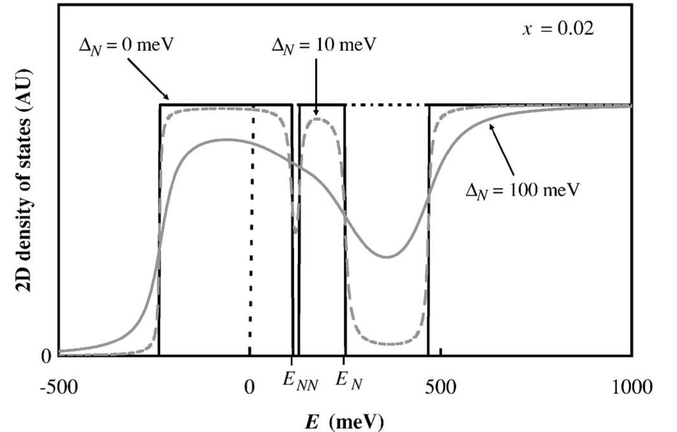

FIG. 2. 2D density of states for GaNAs calculated from the imaginary part of the Green's function using a three-band model (in this calculation, the broadenings on the two energy levels are taken to be equal). The black dotted line shows the GaAs density of states. In the limiting case of all $\Delta_i=0$ meV, the 2D density of states takes the same magnitude as that of the matrix semiconductor although shifted in energy and with band gaps appearing at the impurity energies E_N and E_{NN}.

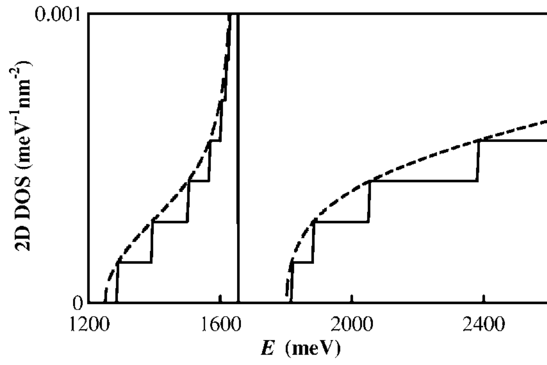

FIG. 3. Calculation for the 2D density of states using the two-band model (with $x=0.01$) for an infinite quantum well of width $d=10$ nm summing over subbands. The dashed line shows the 3D density of states (multiplied by d) for the same nitrogen concentration. The singularity in the 3D case is reproduced as high-energy states in the matrix semiconductor are pushed down below the nitrogen energy.

proaches the energy of the nitrogen state, the condition $\gamma(E)>E_n$ is met for more and more subbands. Thus, the density of states immediately below the nitrogen energy becomes very large as even greater numbers of higher-energy states of the host semiconductor are pushed below it. An important feature of this is that the total number of states in the system is conserved. This can be clearly seen for a single subband and hence follows for the 3D case via the argument of taking $d\to\infty$.

The presence of m_0^*, the matrix semiconductor effective mass, in Eq. (28) is potentially misleading, since it seems to suggest that the effective mass has not changed. The actual effective mass m^*, however, arises out of the dispersion relations, and these remain highly nonparabolic. Specifically, we find $m^*=m_0^* d\gamma(E)/dE$ or, considering Eqs. (9) and (12), $m^*\simeq m_0^*|\alpha_M|^{-2}$. Inspection of Eq. (12) then shows that increasing the broadening will, in general, reduce the increase in effective mass, in accordance with our earlier assertion that the broadening acts to reduce the nonparabolicity.

V. MOBILITY CALCULATIONS FOR TWO- AND THREE-BAND MODELS

Ordinarily in a nonparabolic band, the electron group velocity $v(E)$ would be inversely proportional to $d\gamma(E)/dE$. As just argued in the previous section, in the limit of no broadening, $d\gamma(E)/dE$ is equivalent to $|\alpha_M|^{-2}$, so $v(E)$ may be given approximately by

$$v(E)=|\alpha_M(E)|^2\left(\frac{2\gamma(E)}{m_0^*}\right)^{1/2}. \tag{29}$$

Note that $v(E)$ must be real, so we take it to be zero whenever $\gamma(E)$ is negative (between bands).

So far, we have not discussed how to determine the broadenings on the impurity level. Equation (6) indicates that Δ_j is proportional to the matrix semiconductor density of states at the impurity energy. We assume that the constant of proportionality is the same for all impurity levels, so that given one broadening, we can find any other from the ratio of the densities of states. In the original paper of Wu *et al.*,[31] a broadening of ~100 meV on the isolated nitrogen state (which we label using an N subscript) was found to fit absorption measurements well, so we assume this value for Δ_N. The energy-dependent broadening $\Delta(E)$ can then be found by determining the solution of $f(\Delta)=\Delta-\Sigma_j|\alpha_j(\Delta)|^2\Delta_j=0$. Limiting ourselves to two- and three-band models (in the latter, we incorporate N-N pairs, which we label with an NN subscript), we use the interaction energies V_j and other material parameters for GaN_xAs_{1-x} from Fahy and O'Reilly.[28] Following these authors, we use $x_N=x(1-12x)$ and $x_{NN}=6x^2$ for the impurity concentrations.

We now have all the ingredients in place to calculate the bulk mobility due to nitrogen scattering using

$$\mu_{3D}=-\frac{e}{3}\frac{\int_{-\infty}^{\infty}v^2(E)\tau(E)\frac{df_0(E)}{dE}N_{3D}(E)dE}{\int_{-\infty}^{\infty}f_0(E)N_{3D}(E)dE}, \tag{30}$$

where $f_0(E)$ is the equilibrium distribution function given, in the degenerate case, by the Fermi-Dirac factor (in the nondegenerate case, we may use the Boltzmann factor). Other elastic-scattering processes could be incorporated by simply adding the scattering rates for each process $1/\tau(E)=\Sigma_i 1/\tau_i(E)$. However, for polar optical scattering, the relaxation time approximation is no longer valid and we would have to use a more sophisticated technique for solving Boltzmann's equation such as the ladder method in a nonparabolic band.[37] For now, we consider only the nitrogen-scattering limited mobility.

Firstly, we calculate the relaxation time $\tau(E)$. Figures 4 and 5 show the calculations with $x=0.01$ at temperature $T=300$ K for different input broadenings on the E_N level using a three-band model (the results for the two-band model are similar except that they lack the feature associated with E_{NN}). It should be pointed out that although we have performed these calculations at all energies over a range of 1 eV from the band edge, this includes ranges of energies between the bands. Specifically, the peaks in Fig. 4 occur over the band gaps and are due to the vanishingly small density of states there. From Fig. 1, we can see that as the broadening approaches zero, so does the density of states in the gaps and, hence, the apparent increase in relaxation time over these energies. This, of course, is physically meaningless and does not enter into mobility calculations since the group velocity is zero over these ranges.

The troughs just prior to these peaks occur at the impurity energies and are due to the combined effect of both the density of states and the terms in the summation in Eq. (19) becoming large. This is offset by the fact that the fractional Γ character becomes very small at these energies, which minimizes the drop in the relaxation time. Ignoring the peaks, then, we see that for broadenings in the range 4–100 meV,

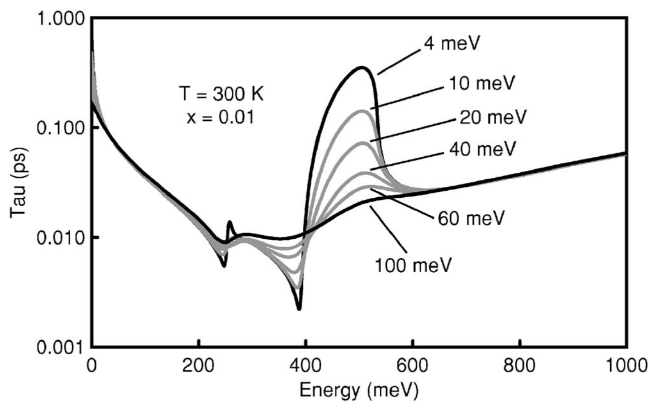

FIG. 4. Energy-dependent relaxation times for different broadenings on the E_N level calculated using the three-band model relative to the band edge. Note that the peaks occur over the energy gaps (due to the density of states vanishing there) and are not featured in mobility calculations.

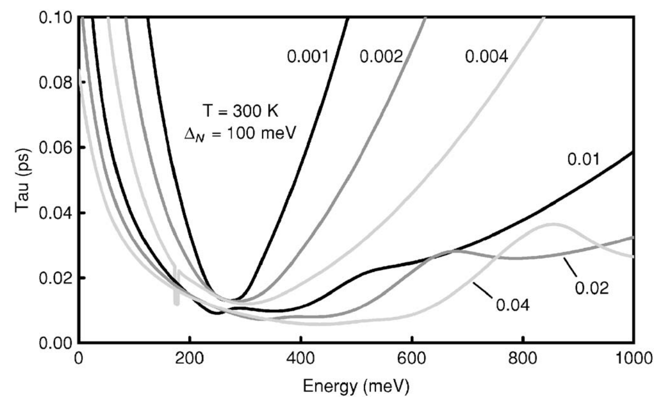

FIG. 6. Energy-dependent relaxation times for different nitrogen concentrations. Here, the energies are given relative to the dilute nitride band edge, although the absolute energies of the band edge will shift down in energy with increasing nitrogen content.

there is little change in the relaxation time, the only effect being a slight increase in $\tau(E)$ near the impurity levels with increasing Δ_N. In Fig. 5, we plot the results for broadenings in the range 100–500 meV. Here, we see an overall increase of $\tau(E)$ with increasing Δ_N. This might appear a little counterintuitive at first, given the earlier interpretation of the scattering as being due to the broadening. However, we see the reason for it in Eq. (19): both the fractional Γ character and the terms in the summation depend on the broadening. While the Γ character increases with increasing Δ_N, it does so at a much slower rate than the decrease in the summation terms. Hence, the scattering rate decreases and $\tau(E)$ increases, in contradiction with the interpretation of Wu *et al.*[34]

Fixing Δ_N at 100 meV, further calculations shown in Figs. 6 and 7 illustrate the effects of varying x and T, respectively. As we would expect, $\tau(E)$ is reduced as we increase the nitrogen concentration. As before, we calculate $\tau(E)$ over all energies, although only the energies in a band are relevant.

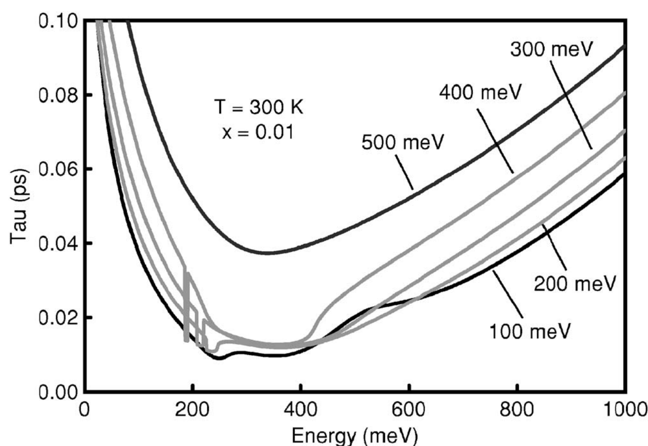

FIG. 5. Energy-dependent relaxation times for large broadenings on the E_N level calculated using the three-band model relative to the band edge. The systematic increase in $\tau(E)$ with larger broadening is due to the reduction of the summation terms in the scattering rate, Eq. (15).

As a general trend, we note that $\tau(E)$ decreases in the lower band and increases in the upper band.

In Fig. 8, we show calculated mobilities using degenerate statistics in comparison to measurements of quantum well structures by Mouillet.[38] At most carrier concentrations, the calculated values are an overestimate. The drop in mobility at higher carrier concentration is due to the Fermi energy being pushed higher into the band where the fractional Γ character, and hence the group velocity, is reduced.

Figure 9 shows the calculated mobility as a function of nitrogen concentration in comparison to measurements by Fowler *et al.*,[39] Mouillet,[38] and Strohm.[40] The Se-doped samples were reported by Fowler *et al.* to exhibit very high carrier concentrations ($\sim 10^{19}$ cm^{-3}), and here, the fit with either the two band (dashed line) or three band (solid line) is good at the measured nitrogen concentrations. Note that the dip in the three-band model curve at around $x=0.006$ absent from the two-band calculations is due to the Fermi energy becoming coincident with the N-N pair energy, where the fractional Γ character is severely reduced. In the measurements by Mouillet, a range of carrier concentrations was found from 5×10^{16} to 2.5×10^{17} cm^{-3}. The calculated mobilities at 10^{17} cm^{-3} are once again an overestimate.

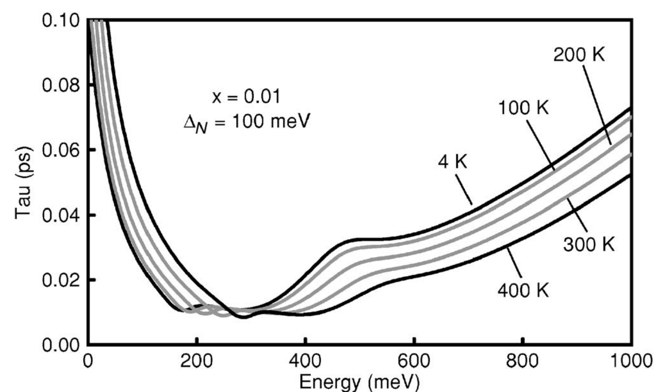

FIG. 7. Energy-dependent relaxation times for different temperatures, relative to the band edge.

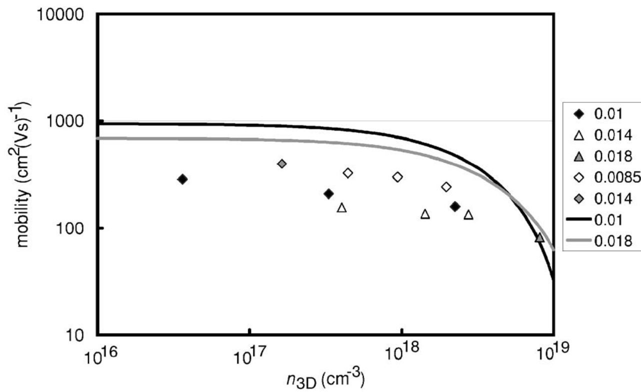

FIG. 8. Room-temperature degenerate mobility as a function of carrier concentration calculated using the three-band model. Results for the two-band model are similar but slightly higher. Data points are measurements of GaNAs quantum well structures by Mouillet (Ref. 38)

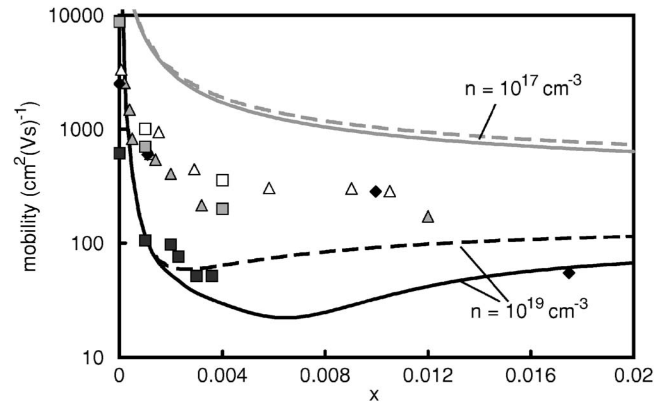

FIG. 9. Room-temperature mobility as a function of nitrogen concentration. The dashed lines are using the two-band model, and the solid lines using the three-band model. The square data points are measured mobilities by Fowler *et al.* (Ref. 39): black, doped with Se ($n \sim 10^{19}$ cm^{-3}); gray, doped with Si; white, doped with B. Triangular points by Mouillet (Ref. 38) ($n \sim 10^{17}$ cm^{-3}) and diamond points by Strohm (Ref. 40) (n not specified).

VI. CONCLUSIONS

Although our calculations show a marked decrease in the mobility from that of GaAs [$\sim$6000 cm^2(V s)$^{-1}$ at room temperature] as nitrogen is added, except in the highly degenerate case, these results are still somewhat larger than the measured mobilities for GaInNAs materials [$\sim$300–400 cm^2(V s)$^{-1}$ for $x \sim 0.01$ at room temperature[3,4]]. At high carrier concentrations, it is the reduction in the fractional Γ character as the Fermi energy moves higher into the band that is responsible for the drop in calculated mobility. We note that Fahy *et al.*[30] find much lower mobilities using their resonant scattering model, although they include many more nitrogen environments than we have in the three-band model. The inclusion of additional cluster states at even lower energies than the N-N pairs would therefore be expected to severely reduce the fractional Γ character and further reduce the mobility. Indeed, Fahy *et al.* argue that these cluster states have crucial significance for the transport properties.

Other factors affecting the mobility not considered here may be polar-optical-phonon, impurity, and defect scatterings. Although in most polar semiconductors, polar-optical-phonon scattering is usually the dominant mechanism limiting the room-temperature mobility, the contribution to the resistivity in GaAs is an order of magnitude smaller than the alloy scattering due to nitrogen centers considered here. Given the consequences of high degeneracy, we would expect ionized impurity scattering to play some role, although this is most significant at low temperature and may be reduced via modulation doping in heterostructures.

Material quality may also be an issue. The formation of dislocation loops during the growth of GaInNAs has been observed using transmission electron microscopy,[41,42] which can lead to the development of threading dislocations, with densities of $(3-4) \times 10^9$ cm^{-2}. Scattering from threading dislocations is known to limit the mobility of bulk GaN to around 140 cm^2(V s)$^{-1}$ at room temperature,[43] although the threading dislocation density in this case is about an order of magnitude greater at around 5×10^{10} cm^{-2}. However, even at the lower dislocation densities reported in GaInNAs, such scattering may still be contributing more to the resistivity of the material than polar-optical-phonon scattering and warrants consideration. As far as we are aware, no specific modeling of the effect of dislocation loops on the mobility has been undertaken.

ACKNOWLEDGMENTS

The authors would like to thank Amalia Patanè for providing early copies of the mobility measurements of Fowler *et al.* (Ref. 41) and Eoin O'Reilly for providing an early proof copy of Ref. 30 This work has been supported by a grant from the Engineering and Physical Sciences Research Council.

*Corresponding author. Electronic address: mpvaug@essex.ac.uk
[1] M. Weyers, M. Sato, and H. Ando, Jpn. J. Appl. Phys., Part 2 **31**, L853 (1992).
[2] M. Kondow, K. Uomi, K. Hosomi, and T. Mozume, Jpn. J. Appl. Phys., Part 2 **33**, L1056 (1994).
[3] C. Skierbiszewski, P. Perlin, P. Wisniewski, T. Suski, W. Walukiewicz, W. Shan, J. W. Ager, E. E. Haller, J. F. Geisz, D. J. Friedman, J. M. Olson, and S. R. Kurtz, Phys. Status Solidi B **216**, 135 (1999).
[4] S. R. Kurtz, A. A. Allerman, C. H. Seager, R. M. Sieg, and E. D. Jones, Appl. Phys. Lett. **77**, 400 (2000).
[5] W. Li, M. Pessa, J. Toivonen, and H. Lipsanen, Phys. Rev. B **64**,

113308 (2001).
[6] J. Teubert, P. J. Klar, W. Heimbrodt, K. Volz, and W. Stolz, IEE Proc.: Optoelectron. **151**, 357 (2004).
[7] R. Mouillet, L. A. de Vaulchier, E. Deleporte, Y. Guldner, L. Travers, and J. C. Harmand, Solid State Commun. **126**, 333 (2003).
[8] D. J. Wolford, J. A. Bradley, K. Fry, and J. Thompson, in *Proceedings of the 17th International Conference on the Physics of Semiconductors*, edited by J. D. Chadi and W. A. Harrison (Springer-Verlag, New York, 1984), p. 627.
[9] X. Liu, M. E. Pistol, L. Samuelson, S. Schwetlick, and W. Seifert, Appl. Phys. Lett. **56**, 1451 (1990).
[10] X. Liu, M. E. Pistol, and L. Samuelson, Phys. Rev. B **42**, 7504 (1990).
[11] D. G. Thomas, J. J. Hopfield, and C. J. Frosch, Phys. Rev. Lett. **15**, 857 (1965).
[12] D. G. Thomas and J. J. Hopfield, Phys. Rev. **150**, 680 (1966).
[13] H. P. Hjalmarson, P. Vogl, D. J. Wolford, and J. D. Dow, Phys. Rev. Lett. **44**, 810 (1980).
[14] L. Bellaiche, S. H. Wei, and A. Zunger, Phys. Rev. B **54**, 17568 (1996).
[15] T. Mattila, S. H. Wei, and Alex Zunger, Phys. Rev. B **60**, R11245 (1999).
[16] P. R. C. Kent and A. Zunger, Phys. Rev. Lett. **86**, 2613 (2001).
[17] P. R. C. Kent and A. Zunger, Phys. Rev. B **64**, 115208 (2001).
[18] P. R. C. Kent, L. Bellaiche, and A. Zunger, Semicond. Sci. Technol. **17**, 851 (2002).
[19] A. Lindsay and E. P. O'Reilly, Solid State Commun. **112**, 443 (1999).
[20] E. P. O'Reilly, A. Lindsay, S. Tomic, and M. Kamal-Saad, Semicond. Sci. Technol. **17**, 870 (2002).
[21] A. Lindsay and E. P. O'Reilly, Physica E (Amsterdam) **21**, 901 (2004).
[22] E. P. O'Reilly, A. Lindsay, and S. Fahy, J. Phys.: Condens. Matter **16**, S3257 (2004).
[23] A. Lindsay and E. P. O'Reilly, Phys. Rev. Lett. **93**, 196402 (2004).
[24] W. Shan, W. Walukiewicz, J. W. Ager III, E. E. Haller, J. F. Geisz, D. J. Friedman, J. M. Olson, and S. R. Kurtz, Phys. Rev. Lett. **82**, 1221 (1999).
[25] A. Lindsay, Ph.D. thesis, University of Surrey, 2002.
[26] S. B. Healy, A. Lindsay, and E. P. O'Reilly, IEE Proc.: Optoelectron. **151**, 397 (2004).
[27] S. Fahy and E. P. O'Reilly, Appl. Phys. Lett. **83**, 3731 (2003).
[28] S. Fahy and E. P. O'Reilly, Physica E (Amsterdam) **21**, 881 (2004).
[29] S. Fahy, A. Lindsay, and E. P. O'Reilly, IEE Proc.: Optoelectron. **151**, 352 (2004).
[30] S. Fahy, A. Lindsay, H. Ouerdane, and E. P. O'Reilly, Phys. Rev. B **74**, 035203 (2006).
[31] J. Wu, W. Walukiewicz, and E. E. Haller, Phys. Rev. B **65**, 233210 (2002).
[32] P. W. Anderson, Phys. Rev. **124**, 41 (1961).
[33] Paul Soven, Phys. Rev. **156**, 809 (1966).
[34] J. Wu, K. M. Yu, and W. Walukiewicz, IEE Proc.: Optoelectron. **151**, 460 (2004).
[35] M. P. Vaughan, Ph.D. Thesis, University of Essex, 2007; B. K. Ridley (unpublished).
[36] M. P. Vaughan and B. K. Ridley, Phys. Status Solidi C **4**, 686 (2007).
[37] M. P. Vaughan and B. K. Ridley, Phys. Rev. B **72**, 075211 (2005).
[38] R. Mouillet, Ph.D. thesis, l'Université Paris V1, 2004.
[39] D. Fowler, O. Makarovsky, A. Patanè, L. Eaves, L. Geelhaar, H. Reichert, and K. Uesugi, in *Physics of Semiconductos*, edited by J. Menéndez and C. G. Van de Valle AIP Conf. Proc. No. 772 (AIP, New York, 2005), p. 497.
[40] E. Strohm, M.Sc. thesis, University of British Columbia, 2002.
[41] M. Herrera, D. Gonzalez, R. Garcia, M. Hopkinson, P. Navaretti, M. Gutierrez, H. Y. Liu, IEE Proc.: Optoelectron. **151**, 385 (2004).
[42] M. Herrera, D. González, J. G. Lozano, R. García, M. Hopkinson, H. Y. Liu, M. Gutierrez, and P. Navaretti, J. Appl. Phys. **98**, 023521 (2005).
[43] D. Zanato, S. Gokden, N. Balkan, B. K. Ridley, and W. J. Schaff, Superlattices Microstruct. **34**, 77 (2003).